APPLIED PHYSICS

10.1126/sciadv.1501690

On-demand transfer of trapped photons on a chip

Ryotaro Konoike, Haruyuki Nakagawa, Masahiro Nakadai, Takashi Asano, Yoshinori Tanaka, Susumu Noda*

Photonic crystal nanocavities, which have modal volumes of the order of a cubic wavelength in the material, are of great interest as flexible platforms for manipulating photons. Recent developments in ultra-high quality factor nanocavities with long photon lifetimes have encouraged us to develop an ultra-compact and flexible photon manipulation technology where photons are trapped in networks of such nanocavities. The most fundamental requirement is the on-demand transfer of photons to and from the trapped states of arbitrary nanocavities. We experimentally demonstrate photon transfer between two nearly resonant nanocavities at arbitrary positions on a chip, triggered by the irradiation of a third nonresonant nanocavity using an optical control pulse. We obtain a high transfer efficiency of ~90% with a photon lifetime of ~200 ps.

INTRODUCTION

Over the past decade, extensive studies have been devoted to on-chip technologies for the manipulation of flying photons, including optical filters (*1*, *2*), optical switches (*3*), and optical quantum circuits (*4*). Recently, we have realized a photonic crystal (PC) nanocavity (*5*) with an ultra-high quality (*Q*) factor of approximately 9,000,000 (*6*) as well as novel photonic structures that enable strong coupling between distant nanocavities on a chip (*7*). Such technologies may enable the manipulation of trapped photons in a network of on-chip photonic nanocavities. Compared to flying photons, trapped photons in PC nanocavities occupy modal volumes of the order of a cubic wavelength in the material. Such strong confinement of photons allows the enhancement of light-matter interactions, leading to single-photon nonlinearity (*8*) or allowing quantum-state manipulation using solid-state cavity quantum electrodynamics (QED) systems (*9*). If trapped photons could be transferred between any nanocavities in a network at arbitrary timings, ultra-compact platforms for the manipulation of photons could be realized, including buffering and switching of both classical and quantum photons (see section SII for details) as well as quantum information processing with single photons and/or cavity QED systems (*10*, *11*). We have previously reported on strong coupling between two distant nanocavities on a chip (*7*). Here, we achieve an important step forward by demonstrating the transfer of trapped photons between two nanocavities on a chip with arbitrary (on-demand) timing by introducing a third control cavity.

The principle of our method for the on-demand transfer of photons is as follows. We consider the system shown in Fig. 1A, where photons trapped in cavity A are transferred to cavity B through a third control cavity C placed between cavities A and B. The resonant frequencies of cavities A and B are detuned ($\omega_A < \omega_B$) such that Rabi oscillation between them is suppressed (see Fig. 1B). The resonant frequency of cavity C is initially set to be much lower than those of cavities A and B ($\omega_C << \omega_A < \omega_B$). In this situation, one eigenmode of the system has the field distribution close to cavity A, as shown in the left-hand inset (I) of Fig. 1B. When we inject photons into this eigenmode, most of the photons are initially trapped in cavity A. We then greatly increase the frequency of cavity C such that the condition ($\omega_A < \omega_B << \omega_C$) is satisfied. If the change in frequency of cavity C is slow enough (that is, adiabatic) to prevent scattering of the photons to the other existing modes, the wave function moves along the yellow line shown in Fig. 1B until, finally, most of the photons become trapped in cavity B, as shown in the right-hand inset (III) of Fig. 1B. Thus, the trapped photons in cavity A are transferred to cavity B by tuning the frequency of cavity C. This method is based on the coherent process in which photons stay in the same eigenmode during the entire process and is even applicable to a single photon (*12*). The frequency of cavity C can be varied using the carrier plasma effect (*13*) by irradiating it with a laser pulse. This method makes use of the fact that the probability of photons existing in cavity C is much lower than that in cavities A and B in this coupled system, as seen in the insets of Fig. 1B. Thus, even if free carriers are used to induce a frequency change of cavity C, photons are not absorbed, which leads to high transfer efficiency. Below, we experimentally demonstrate this prediction for the first time.

RESULTS

We fabricated a two-dimensional silicon PC sample containing three nanocavities, a microscope image of which is shown in Fig. 1C. The design of each nanocavity is based on a multiheterostructure cavity (*14*), as shown in Fig. 1D. Each nanocavity was separated from its neighbor by 41 μm, and the three were connected by intermediate waveguides. An independent microheater made of Au/Ti was placed at a distance of ~10 μm from each nanocavity to tune the resonances. From spectrum measurements, we obtained a *Q* factor of the fabricated nanocavities of approximately 400,000. The resonant wavelengths of the three nanocavities typically had fluctuations of less than 1 nm as a result of fabrication error. To confirm the initial resonant wavelengths and coupling strengths of the nanocavities, we measured spectra while varying the power (P_B) input to heater B, which is close to cavity B. The results are shown in Fig. 2A. The peaks in the spectra correspond to the eigenmode frequencies of the system. We fitted the measured positions of the peaks (shown in Fig. 2B as red crosses) as a function of heater power with the eigenmode wavelengths calculated by coupled mode theory (CMT) (*15*) to determine the original wavelengths and coupling strengths of the three nanocavities. The method used in the

Department of Electronic Science and Engineering, Kyoto University, Kyoto 615-8510, Japan.
*Corresponding author. Email: snoda@kuee.kyoto-u.ac.jp

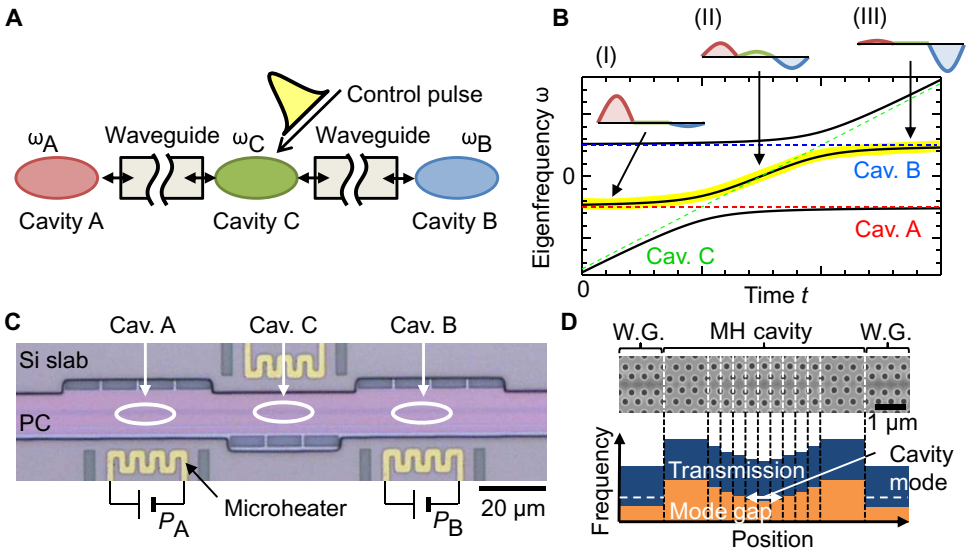

Fig. 1. Device structure and the scheme. (**A**) Schematic illustration of our system for on-demand transfer of photons in a PC. Two nanocavities that trap photons (cavities A and B) are indirectly coupled by a third control nanocavity (cavity C). (**B**) Temporal change of the eigenmode frequencies (solid lines) and resonant frequencies of cavities A, B, and C (red, blue, and green dashed lines, respectively) where the frequency of cavity C is modulated. The insets show the energy concentrations of the central eigenmodes of cavities A, B, and C before and after modulation. (**C**) Microscope image of a fabricated sample in which three nanocavities are formed on a silicon PC slab together with three microheaters. (**D**) Scanning electron microscopy image and the spatial band structure of the fabricated nanocavity. MH, multiheterostructure; W.G., waveguide.

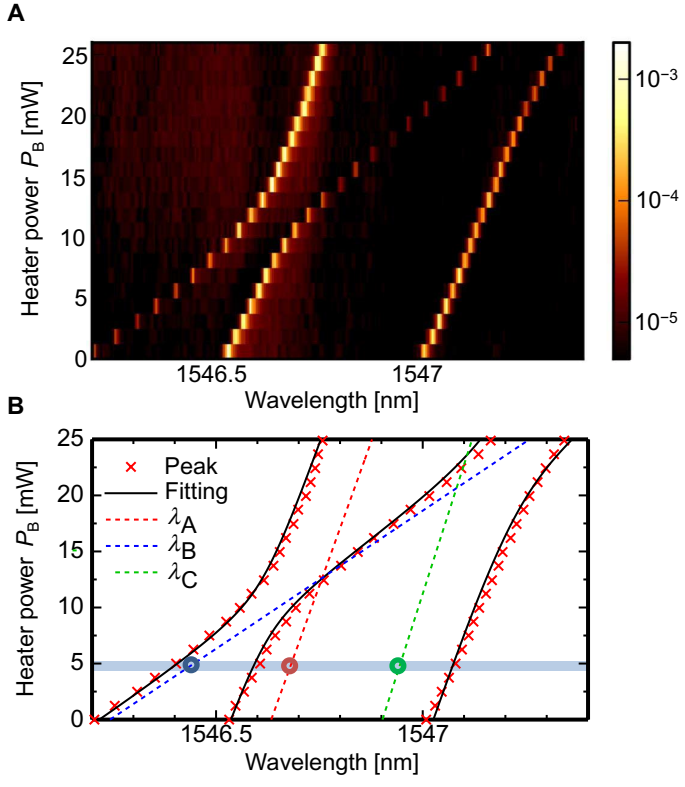

Fig. 2. Measurement of the eigenmode wavelengths. (**A**) Resonant spectra of the system measured while varying the input power to heater B. (**B**) Fits (solid lines) to the extracted peak positions (red crosses) of the spectra, plotted together with the original resonant wavelengths of cavities A, B, and C (red, blue, and green dashed lines, respectively).

fitting process is described in section SIII. Figure 2B shows the fits (black solid lines) and the original resonant wavelengths of cavities A, B, and C (red, blue, and green dashed lines, respectively). From the fits, we estimated that if cavities A and C (B and C) are set to be in resonance, they potentially have the coupling strength of ~25 GHz (~16 GHz). Because these values are much larger than the rate of dissipation of the system (~500 MHz, which is obtained from the *Q* factor), the cavities potentially exhibit strong coupling (*7*) if they are in resonance, which is needed to form the eigenmodes in Fig. 1B. We note that in the experiments, Rabi oscillation does not occur because the cavities are detuned, and only the highlighted eigenmode in Fig. 1B is populated throughout the operation (details are shown in section SIV together with a similar analysis using either heater A or C). Here, if we set P_B = 4.8 mW (indicated by the blue horizontal line in Fig. 2B), we can see that the cavities are detuned from each other, and the initial condition in Fig. 1B is approximately reproduced. We further adjusted the resonances by inputting power P_A = 2.0 mW to heater A in addition to P_B = 4.8 mW.

Figure 3 shows a schematic illustration of the experimental setup. A pulsed pump laser with a wavelength of 820 nm and a pulse duration of 140 fs was used together with an optical parametric oscillator (OPO) system to generate synchronized signal (1547 nm) and control (820 nm) pulses. Reference pulses for the time-resolved measurement (*16*) were split from the signal pulses. Both the signal and reference pulses were filtered using optical band-pass filters to obtain time durations of approximately 20 and 4 ps, respectively. The signal pulses were then input to the sample from the left-hand side of cavity A to excite the system. The center wavelength of the signal pulses matched the initial resonant wavelength of the central eigenmode (cavity A), and the spectral width was narrow compared to the frequency spacing between the central eigenmode and the other eigenmodes. Therefore, the signal pulse selectively excites cavity A, and after the excitation, the

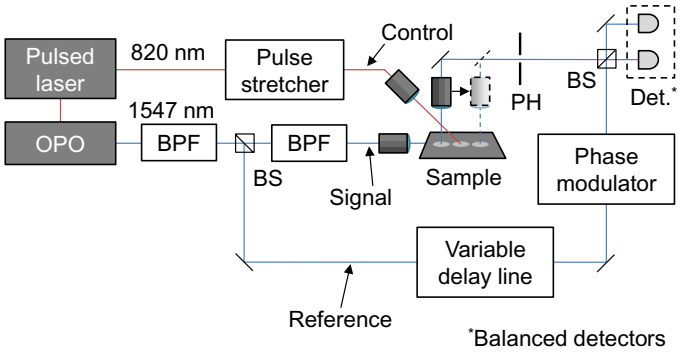

Fig. 3. Setup of the time-resolved measurement. Schematic illustration of the experimental setup for time-resolved measurements. BS, beam splitter; PH, pinhole; BPF, band-pass filter.

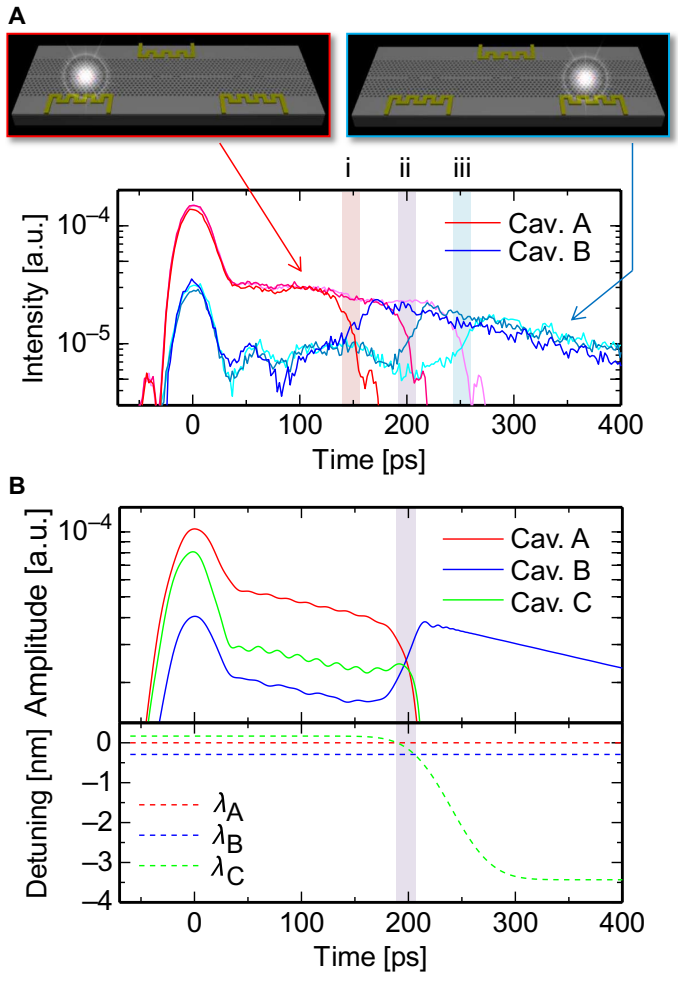

Fig. 4. Experimental on-demand transfer of trapped photons. (**A**) Experimental results for the on-demand transfer of trapped photons between cavities A and B (red and blue solid lines, respectively) with irradiation of cavity C by an optical control pulse at three different timings (i, ii, and iii). Cavity A is excited at 0 ps, and the photons are transferred to cavity B at arbitrary timings with the maximum transfer efficiency of 90%. (**B**) Results of a numerical simulation based on CMT, using the experimental parameters. a.u., arbitrary units.

photons are trapped here. At any timing after this excitation, we can irradiate cavity C using a control light pulse with a spot size of several micrometers to induce the transfer of photons (Fig. 1B). The control pulse is absorbed by the substrate to generate free carriers with a density of approximately 1×10^{19} cm^{-3}, yielding a change of ~0.2% in the refractive index around cavity C. This gives a perturbative change that blue-shifts the resonant wavelength of cavity C by ~3 nm. Because this change in the dimensions of cavity C induced by the irradiation of the control pulse is small, it does not affect the overall performance. The time duration of the control pulses was increased to 71 ps before the irradiation to the sample by using a pulse stretcher. This pulse length allows the adiabatic condition ($\alpha << \mu^2$) to be satisfied in our sample, where α is the rate of change in the angular frequency of cavity C and μ is the coupling strength between adjacent nanocavities. The blue shift of cavity C was retained for several nanoseconds, corresponding to the carrier lifetime of the Si PC (*16*). Because this value is much longer than the photon lifetime of the coupled nanocavity system (several hundred picoseconds), we can assume that free carriers do not decay during the photon lifetime. We collected photons dropped from cavity A using an objective lens and a pinhole. Time-resolved measurements of cavity A were performed by measuring both the dropped and the reference photons. We then moved the objective lens to collect photons from cavity B and performed the same measurement. The time resolution was determined by the reference pulse duration and was approximately 4 ps.

We performed the transfer experiments using control pulses with three different timings. The experimental results are plotted in Fig. 4A. Here, the three red (blue) lines show the time-resolved amplitudes of cavity A (B) corresponding to the three control timings (i, ii, and iii). These results clearly show that the light trapped in cavity A by the excitation at 0 ps was transferred to cavity B at each control timing (i, 150 ps; ii, 200 ps; and iii, 250 ps). Here, the pulsed signals at 0 ps correspond to the scattered part of the input light pulse and are not essential. Figure 4B shows the results of a numerical simulation based on temporal CMT using the experimental parameters. The simulations are in agreement with the experimental results (Fig. 4A), implying that we have successfully demonstrated the on-demand transfer of trapped photons between two nanocavities on a chip. The intrinsic lifetime of the trapped photons in the system was approximately 200 ps. This value can be improved by using more precise fabrication processes, leading to fewer structural errors. From the results of the simulation (Fig. 4B), we determined the initial energy concentrations in cavities B and C, which were 15 and 29% of that of cavity A, respectively. The reason for the initial distribution of photons in cavities B and C can be explained as follows. As shown in Fig. 4B, the resonant wavelength of cavity C is initially very close to that of cavity A. Because of this, the eigenmode in which photons exist deviated slightly from cavity A, and it distributed a small fraction of photons in cavities B and C. Theoretically, this can be suppressed by making the initial detuning of cavities B and C larger with respect to cavity A (*12*). In the experimental results of Fig. 4A, we consider that most of the photons, including those existing in cavities B and C, are adiabatically transferred to cavity B. Using this assumption, we calculated the ratio of the energy transferred to cavity B from cavity A only to the initial energy in cavity A, which we define here as the transfer efficiency. We eliminated the effect of the intrinsic photon lifetime in our calculation. The resulting maximum transfer efficiency obtained from our experimental results is 90% (see section SV for

details). This value is in agreement with our previous theoretical prediction (*12*), which implies that this scheme genuinely facilitates on-demand photon transfer. Detailed arguments supporting this conclusion are given in sections SV and SVI.

DISCUSSION

We have demonstrated the on-demand transfer of trapped photons, which can pave the way to ultra-compact platforms that manipulate photons on a chip. Our scheme can be scaled up to a large number of cavities in principle (see section SII). We have used optical control pulses to perform the transfer of photons in this paper. However, we consider that it is also possible to use electric control of the local refractive index (*17*), which can be integrated on the same silicon chip. In this context, fully on-chip platforms for the manipulation of trapped photons can be expected. Our demonstration would lead to flexible platforms that manipulate trapped photons on a chip, which has many applications including buffering and switching of classical/quantum photons as well as quantum information processing.

MATERIALS AND METHODS

Sample design and fabrication

We formed a triangular-lattice two-dimensional PC structure on a silicon-on-insulator substrate, where the top Si layer had a thickness of 220 nm. Details for the design of the PC nanocavities are described in section SI. Electron-beam lithography and dry etching techniques were used to form the PC structure. After that, Ti (25 nm) and Au (80 nm) were deposited to form the microheaters. Finally, wet etching with hydrogen fluoride was performed to form the air-clad PC slab structure, where the metal parts were covered by a photoresist (AZ) to prevent damages.

Spectrum measurements

For the measurement of the transmission spectra of the system (Fig. 2A), we input light from a tunable continuous wave laser (Santec TSL-210V). The wavelength was measured using a wavelength meter (Agilent 86122A), and the transmitted power was measured using an optical chopper (NF 5584A) and a lock-in amplifier (NF 5600A). The wavelength resolution of the measurement setup was ~0.3 pm.

Time-resolved measurements

For the time-resolved measurements, we used a pulsed laser (Coherent Chameleon Ultra II) for the pump in Fig. 3. The pump pulses had a duration of 140 fs, a wavelength of 820 nm, and a repetition rate of 80 MHz. An OPO (Chameleon Compact OPO) was used to generate 1547-nm signal pulses. The signal pulses were filtered to have a rectangular spectrum with a width of 1.0 nm. We picked up pulses with a repetition rate of 5 MHz using an acousto-optic modulator and an electro-optic modulator for the pump and signal pulses, respectively. We then split the signal pulses into input pulses, which were further filtered to generate a Gaussian shape with a 0.2-nm full width at half maximum, and reference pulses for the cross-correlation measurement. The input pulses were focused on the cleaved edge of the excitation waveguide of the sample. The reference pulses were passed through a variable delay line and an electro-optic phase modulator (a ramped function from 0 to 2π was applied with a frequency of 179 kHz). The photons dropped from each cavity were collected using an objective lens (numerical aperture, 0.4) and were measured using balanced homodyne detection with the reference pulses. The output electronic signal of the detector was then measured using a lock-in amplifier (Zurich Instruments HF2LI). Control pulses, which were split from the pump pulses, were stretched to have a pulse width of 71 ps by adding a group velocity dispersion of ~10 ps/nm using a pair of optical gratings. The control pulses with an energy of ~36 pJ per pulse were then focused on cavity C with a spot size of a few micrometers to induce light transfer. In our experiments, the color of the signal pulses was dynamically changed by the modulation of cavity C. We made sure that the reference pulses contain the two wavelengths of the signal photons before and after the transfer. Here, we set the spectral shape of the reference pulses to be rectangular with a width of 1.0 nm to measure all the photons during the operation (the change in wavelength was approximately 0.3 nm).

SUPPLEMENTARY MATERIALS

Supplementary material for this article is available at http://advances.sciencemag.org/cgi/content/full/2/5/e1501690/DC1

I. Design of the PC nanocavity
II. Theoretical proposal of a scheme for large-scale applications
III. Fitting of spectra measured by heating cavity B
IV. Discussions about the coupling strength and the spectrum measurements on supplying power to heaters A and C
V. Calculations of transfer efficiency and its correction
VI. Experimental verification of a system with two cavities
table S1. Fitted parameters corresponding to experimental peak shifts as a function of heater power.
table S2. Fitted heating slope (efficiency) of each cavity.
table S3. Fitted parameters and transfer efficiencies determined from experiments.
table S4. Values of *r* obtained from measured spectra.
fig. S1. Design of the PC waveguide.
fig. S2. Design of the PC nanocavity.
fig. S3. Schematic illustration of a photon buffer system.
fig. S4. Single-bit shift operation.
fig. S5. Results of a numerical simulation of the 1-bit shift.
fig. S6. Results of a numerical simulation in which 6-bit units are connected in series.
fig. S7. Schematic representations of the sample.
fig. S8. Shifts of the eigenmodes by heaters A and C.
fig. S9. Measured optical Rabi oscillation.
fig. S10. Correction of the transfer efficiency.
fig. S11. Coupling efficiencies and *Q* factors of the cavities.
fig. S12. Schematic illustrations of photon transfer with two cavities.
fig. S13. Spectra measured while varying the detuning by local thermal oxidation.
fig. S14. Experimental results for photon transfer in the system where two nanocavities are coupled.
fig. S15. Schematic representation of a model of the two-cavity system.
References (*18*–*20*)

REFERENCES AND NOTES

1. H. Takahashi, S. Suzuki, K. Kato, I. Nishi, Arrayed-waveguide grating for wavelength division multi/demultiplexer with nanometre resolution. *Electron. Lett.* **26**, 87–88 (1990).
2. H. Takano, Y. Akahane, T. Asano, S. Noda, In-plane-type channel drop filter in a two-dimensional photonic crystal slab. *Appl. Phys. Lett.* **84**, 2226–2228 (2004).
3. Y. Vlasov, W. M. J. Green, F. Xia, High-throughput silicon nanophotonic wavelength-insensitive switch for on-chip optical networks. *Nat. Photonics* **2**, 242–246 (2008).
4. A. Politi, M. J. Cryan, J. G. Rarity, S. Yu, J. L. O'Brien, Silica-on-silicon waveguide quantum circuits. *Science* **320**, 646–649 (2008).
5. S. Noda, A. Chutinan, M. Imada, Trapping and emission of photons by a single defect in a photonic bandgap structure. *Nature* **407**, 608–610 (2000).
6. H. Sekoguchi, Y. Takahashi, T. Asano, S. Noda, Photonic crystal nanocavity with a *Q*-factor of ~9 million. *Opt. Express* **22**, 916–924 (2014).
7. Y. Sato, Y. Tanaka, J. Upham, Y. Takahashi, T. Asano, S. Noda, Strong coupling between distant photonic nanocavities and its dynamic control. *Nat. Photonics* **6**, 56–61 (2012).

8. M. Soljačić, J. D. Joannopoulos, Enhancement of nonlinear effects using photonic crystals. *Nat. Mater.* **3**, 211–219 (2004).
9. T. Yoshie, A. Scherer, J. Hendrickson, G. Khitrova, H. M. Gibbs, G. Rupper, C. Ell, O. B. Shchekin, D. G. Deppe, Vacuum Rabi splitting with a single quantum dot in a photonic crystal nanocavity. *Nature* **432**, 200–203 (2004).
10. H. J. Kimble, The quantum internet. *Nature* **453**, 1023–1030 (2008).
11. M. Yamaguchi, T. Asano, Y. Sato, S. Noda, Photonic quantum computation with waveguide-linked optical cavities and quantum dots (2011).
12. R. Konoike, Y. Sato, Y. Tanaka, T. Asano, S. Noda, Adiabatic transfer scheme of light between strongly coupled photonic crystal nanocavities. *Phys. Rev. B* **87**, 165138 (2013).
13. S. F. Preble, Q. Xu, M. Lipson, Changing the colour of light in a silicon resonator. *Nat. Photonics* **1**, 293–296 (2007).
14. Y. Tanaka, T. Asano, S. Noda, Design of photonic crystal nanocavity with *Q*-factor of ~10^9. *J. Lightwave Technol.* **26**, 1532–1539 (2008).
15. C. Manolatou, M. J. Khan, S. Fan, P. R. Villeneuve, H. A. Haus, J. D. Joannopoulos, Coupling of modes analysis of resonant channel add-drop filters. *IEEE J. Quant. Electron.* **35**, 1322–1331 (1999).
16. J. Upham, Y. Tanaka, Y. Kawamoto, Y. Sato, T. Nakamura, B. S. Song, T. Asano, S. Noda, Time-resolved catch and release of an optical pulse from a dynamic photonic crystal nanocavity. *Opt. Express* **19**, 23377–23385 (2011).
17. T. Tanabe, K. Nishiguchi, E. Kuramochi, N. Masaya, Low power and fast electro-optic silicon modulator with lateral *p-i-n* embedded photonic crystal nanocavity. *Opt. Express* **17**, 22505–22513 (2009).
18. Y. Tanaka, J. Upham, T. Nagashima, T. Sugiya, T. Asano, S. Noda, Dynamic control of the *Q* factor in a photonic crystal nanocavity. *Nat. Mater.* **6**, 862–865 (2007).
19. Y. Takahashi, Y. Inui, M. Chihara, T. Asano, R. Terawaki, S. Noda, A micrometer-scale Raman silicon laser with a microwatt threshold. *Nature* **498**, 470–474 (2013).
20. H. S. Lee, S. Kiravittaya, S. Kumar, J. D. Plumhof, L. Balet, L. H. Li, M. Francardi, A. Gerardino, A. Fiore, A. Rastelli, O. G. Schmidt, Local tuning of photonic crystal nanocavity modes by laser-assisted oxidation. *Appl. Phys. Lett.* **95**, 191109 (2009).

Acknowledgments: We thank J. Gelleta for useful discussions. **Funding:** This paper is partially based on results obtained from a project supported by the New Energy and Industrial Technology Development Organization. R.K. acknowledges support from a research fellowship of the Japan Society for the Promotion of Science. **Author contributions:** S.N. supervised the whole project with T.A. and Y.T. R.K. designed and fabricated the samples, performed the experiments, and analyzed the data with H.N., M.N., T.A., and Y.T. S.N., R.K., T.A., H.N., M.N., and Y.T. discussed the results and wrote the paper. **Competing interests:** The authors declare that they have no competing interests. **Data and materials availability:** All data needed to evaluate the conclusions in the paper are present in the paper and/or the Supplementary Materials. Additional data related to this paper may be requested from the authors.

Submitted 23 November 2015
Accepted 26 April 2016
Published 20 May 2016
10.1126/sciadv.1501690

Citation: R. Konoike, H. Nakagawa, M. Nakadai, T. Asano, Y. Tanaka, S. Noda, On-demand transfer of trapped photons on a chip. *Sci. Adv.* **2**, e1501690 (2016).

Science Advances

On-demand transfer of trapped photons on a chip

Ryotaro Konoike, Haruyuki Nakagawa, Masahiro Nakadai, Takashi Asano, Yoshinori Tanaka and Susumu Noda

Sci Adv **2** (5), e1501690.
DOI: 10.1126/sciadv.1501690